The flow of conducting fluids in circular pipes under transverse magnetic fields

By J. A. SHERCLIFF
Department of Engineering, University of Cambridge

(*Received* 19 *September* 1956)

SUMMARY

The flow rate of liquid metals is commonly measured by electromagnetic flowmeters. In these the fluid moves through a region of transverse magnetic field, inducing a potential difference between two electrodes on the walls of the pipe. The ratio of signal to flow rate is dependent on the velocity profile, and this is affected by electromagnetic forces.

In this paper the ultimate steady velocity profile and its associated pressure gradient and induced potential are calculated for the case of laminar flow in a circular pipe whose walls are conducting but without contact resistance. Laminar flow is encouraged by a transverse field. When the fluid conductivity and field strength are sufficiently high, boundary layers occur with a thickness inversely proportional to normal field intensity. The induced potential difference is then 0·926 of the value corresponding to the case of uniform velocity if the walls are non-conducting.

The distance the fluid must travel after entering the transverse field before the steady state is reached is next estimated by a Rayleigh approximation. The inlet velocity is taken to be uniform and effects which occur at the edge of the field are neglected. The process falls into two stages, first a boundary-layer growth and then an adjustment of the velocity away from the walls, occupying a much greater length of pipe. The entry length is shorter than it is in the case of flow in a rectangular pipe, but is still too long for appreciable distortion of the velocity profile to occur within practical flowmeters except at low flow rates. The pressure drop associated with the adjustment of the velocity profile is found to be independent of field strength, if this is high, and about one-eighth of the drop which occurs in the non-conducting case.

Experiments are described in which steady-state pressure gradients and induced potential differences were measured in mercury flowing along Perspex pipes of 0·5 and 0·25 in. bore in transverse fields up to 14500 gauss. The results confirmed the steady-state theory within the limitations of experimental

accuracy and the assumption in the theory of high conductivity and an intense field. The experiments also covered the entry region in many cases, and showed that the theoretical entry lengths were correct in order of magnitude but over-estimated. However, the exact entry condition was uncertain, and steady readings were difficult to obtain in the entry region.

1. Introduction

The rate of flow of a liquid may be measured by passing it along a pipe under a transverse magnetic field. The potential difference induced between two electrodes situated at the ends of a diameter of the pipe perpendicular to the flow and to the field may then be used to indicate the flow rate.

The ratio of the induced potential difference to the flow rate is affected by several factors, including the conductivity of the pipe walls and the form of the velocity profile. If the pipe is circular, the induced potential difference for a given flow rate is insensitive to the form of the velocity profile, provided the velocity is dependent only on distance from the axis of the pipe (Kolin 1945). This is usually the case for laminar or turbulent flow in the absence of upstream disturbances. If the profile departs from radial symmetry, the ratio of potential difference to flow rate can vary very widely (Shercliff 1954, 1955).

If the liquid is a good conductor and the magnetic field is sufficiently strong, the velocity profile can be appreciably distorted by electromagnetic forces (Hartmann 1937, Shercliff 1953), and the induced potential seriously affected. This can occur when electromagnetic flowmeters are used with mercury or liquid sodium.

The full distortion of an entry profile by a transverse field takes place over an entry length, which may be large or small in comparison with the distance the fluid traverses between the onset of the transverse field and the electrodes. The transverse field cannot have an abrupt edge, but nevertheless may change rapidly from negligible proportions to a high uniform intensity.

This paper examines theoretically the steady state of laminar flow in a circular pipe under a transverse field and, by means of a Rayleigh approximation, the entry length necessary to achieve it. Experiments are described which support the theoretical conclusions.

There is considerable interest in laminar flow since it persists at high Reynolds numbers in the presence of a transverse field (Murgatroyd 1953, Lock 1955). The experiments described include cases of laminar and turbulent flow.

In addition to the effect of a uniform transverse field on the velocity profile, there is another distorting effect due to secondary currents where the fluid enters the region of transverse field. This effect is ignored in the present analysis.

2. Governing equations

As figure 1 shows, we select Cartesian axes (x, y, z) such that the z-axis lies along the axis of the pipe, and the x-axis is parallel to the imposed uniform field H_0 existing outside the pipe.

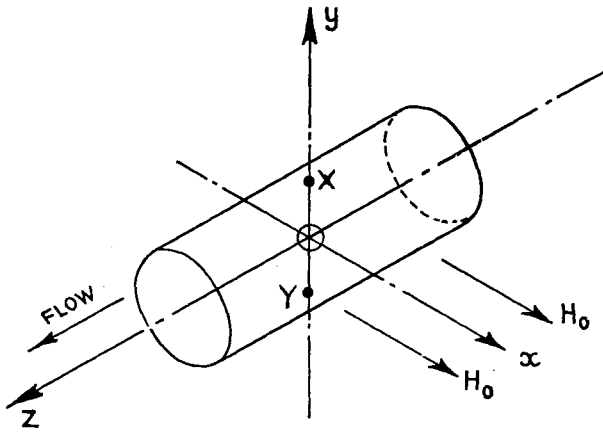

Figure 1. Axes and electrodes.

Various authors (e.g. Bullard 1955) have derived the basic equations for the motion of conducting fluids, pointing out that the displacement current and the convection of charges are negligible. In electromagnetic units Maxwell's equations therefore become

$$\operatorname{curl}\mathbf{E} = -\mu\,\partial\mathbf{H}/\partial t \tag{1}$$

and

$$\operatorname{curl}\mathbf{H} = 4\pi\mathbf{j}, \tag{2}$$

in which $\mathbf{E}$, $\mathbf{H}$ and $\mathbf{j}$ are the electric field, magnetic field and current density vectors respectively, and μ is the permeability of the fluid. Ohm's law requires that

$$\mathbf{j} = \sigma(\mathbf{E} + \mu\mathbf{v}\times\mathbf{H}), \tag{3}$$

in which $\mathbf{v}$ is the fluid velocity and σ is the fluid conductivity. The dynamical equation is

$$\mu\mathbf{j}\times\mathbf{H} + \eta\nabla^2\mathbf{v} - \operatorname{grad}p = \rho\{\partial\mathbf{v}/\partial t + (\mathbf{v}\,.\,\operatorname{grad})\mathbf{v}\}, \tag{4}$$

in which p, ρ and η are the fluid pressure, density and viscosity respectively. We assume that ρ is constant, and μ is unity in both the fluid and the pipe walls. Consequently

$$\operatorname{div}\mathbf{v} = 0, \quad \text{and} \quad \operatorname{div}\mathbf{H} = 0. \tag{5}$$

For the motion of fluid in a straight pipe under a uniform transverse field, where conditions may vary in time but not in the z-direction (apart from the pressure gradient), the equations become linear in the unknown quantities. Differentiation of (4) with respect to z shows that $\operatorname{grad}(\partial p/\partial z)$ vanishes, and hence that $\partial p/\partial z$ is a function of time only. It is compatible with the above equations, and with the boundary conditions, for v_x, v_y

and H_y to vanish and H_x to have the constant value H_0. Equations (1) to (5) then reduce to two equations in the unknown components H_z and v_z:

$$\nabla^2 H_z + 4\pi\mu\sigma H_0 \partial v_z/\partial x = 4\pi\mu\sigma \partial H_z/\partial t \tag{6}$$

and

$$\eta\nabla^2 v_z + (\mu H_0/4\pi)\partial H_z/\partial x = \partial p/\partial z + \rho \partial v_z/\partial t. \tag{7}$$

The Laplacian operators comprise two derivatives only.

The estimation of the entry length for velocity-profile distortion to occur after entry into a transverse field is a non-linear problem, as it stands. There is, however, an obvious analogy with the above linear case, in which there is variation with time instead of with z. We should therefore expect results of the right order if we calculate settling times in the linear problem, and convert these to entry lengths by multiplying by v_0, the mean velocity of flow in the pipe, which is necessarily constant. The variables z and t will be measured from the onset of the transverse field.

The equations (6) and (7) can be expressed non-dimensionally by means of the substitutions

$$v = v_z/v_0, \qquad h = H_z/4\pi v_0(\sigma\eta)^{1/2}, \qquad P = -(a^2/\eta v_0)\partial p/\partial z,$$
$$X = x/a, \qquad Y = y/a, \qquad T = \eta t/\rho a^2,$$
$$M = \mu H_0 a(\sigma/\eta)^{1/2}, \quad \text{and} \quad \beta = 4\pi\mu\sigma\eta/\rho,$$

where a is the internal radius of the pipe. We then have

$$\Delta h + M \partial v/\partial X = \beta \dot{h} \tag{8}$$

and

$$\Delta v + M \partial h/\partial X + P = \dot{v}, \tag{9}$$

in which $\Delta = \partial^2/\partial X^2 + \partial^2/\partial Y^2$, and a dot denotes differentiation with respect to T.

The dimensionless fluid property β is of the order of 10^{-6} for liquid metals. We shall therefore neglect the β-term in (8). This may be shown to be justified except at unusually large values of M, which is of the order of 10^2 in practical flowmeters. The role of h is now limited to that of a current stream-function, since

$$j_y = -v_0(\sigma\eta)^{1/2}\partial h/\partial x, \quad \text{and} \quad j_x = v_0(\sigma\eta)^{1/2}\partial h/\partial y. \tag{10}$$

In view of the interest in flowmeters, it is necessary to consider the electric potential V induced by the motion. This potential exists, because neglecting $\dot{h}$ implies that curl $\mathbf{E}$ is negligible. Then $\mathbf{E} = -\text{grad}\, V$, and from (3) it follows that

$$\partial V/\partial y = \mu H_0 v_z - j_y/\sigma. \tag{11}$$

It is convenient to express the flowmeter output V_{XY}, measured between the electrodes X and Y (figure 1), in terms of a sensitivity S, where

$$S = V_{XY}/2\mu H_0 a v_0. \tag{12}$$

This takes the value unity for uniform or radially-symmetric velocity profiles in a non-conducting circular pipe (Kolin 1945).

Spatial boundary conditions

One obvious condition is that v_z and v shall vanish at the wall. The other condition concerns the magnetic field and potential. In the absence of any contact resistance between the fluid and the walls, the potential is everywhere continuous. Also H_z and h must be continuous at the fluid-wall interface and zero at the exterior of the walls. This secures continuity of current flow between the fluid and the walls, and precludes the flow of current outside the walls. Any voltage measuring device would take a negligibly small current.

From (10) it follows that j_0, the total wall current per unit length of pipe, is equal to $(\sigma\eta)^{1/2}v_0 h$, in which h is taken at the fluid boundary. If *as* and *an* indicate distances along the boundary and inward normal respectively, as shown in figure 2, and we assume that the wall has conductivity σ_0 and

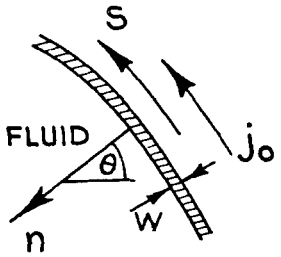

Figure 2. Portion of wall.

thickness w ($\ll a$), then $-j_0/w\sigma_0 = (\partial V/\partial s)/a$, V being in the wall or in the fluid at the wall. At the wall, v vanishes and $-\sigma \operatorname{grad} V = \operatorname{curl} \mathbf{H}/4\pi$, and hence $\partial V/\partial s = -(\eta/\sigma)^{1/2}v_0 \partial h/\partial n$. Eliminating $\partial V/\partial s$ and j_0, we see that at the fluid boundary

$$h = \frac{w\sigma_0}{a\sigma}\frac{\partial h}{\partial n}, \tag{13}$$

the other spatial boundary condition, if contact resistance is negligible. We shall write c for $w\sigma_0/a\sigma$, a dimensionless quantity.

In all that follows, complete symmetry in the x and y axes will prevail, with the result that v is even in X and Y, and that h is odd in X and even in Y.

3. The steady state solution

In an earlier paper (Shercliff 1953), (6) and (7) were solved for the case of steady flow in a rectangular channel with non-conducting walls. It was found that, when M is large, a core of uniform velocity occurs together with boundary layers at the walls. We should therefore expect similar behaviour in a circular pipe with thin conducting walls, the case which is now analysed.

We make the following assumptions.

(i) M is large in comparison with unity.

(ii) The boundary layer thickness is much smaller than the pipe radius, so that all variables may be treated locally as functions only of the distance an from the wall.

(iii) P is of the same order as Mv, as in the rectangular case, when M is large. P is here a constant, and v is of order unity.

(iv) In the core, Δv is negligible in (9), signifying that viscous forces are negligible.

The boundary layer region

The application of assumption (ii) to (8) and (9) for a point on a radius vector inclined at an angle θ to the x-axis (see figure 2) yields the equations

$$h'' - mv' = v'' - mh' + P = 0, \tag{14}$$

in which $m = M\cos\theta$, and dashes denote differentiations with respect to n. The boundary conditions are that $v = 0$ and $h = ch'$ when $n = 0$, and that v and h must become relatively steady outside the layer, approaching the local core values v_c and h_c. The solution is

$$v = v_c\{1 - \exp(-mn)\}, \tag{15}$$

$$h = h(0) - v + Pn/m. \tag{16}$$

The boundary-layer thickness is of the order of $1/m$, which is proportional to the reciprocal of the normal field intensity. The last term in (16) is negligible except where θ approaches $\frac{1}{2}\pi$, by virtue of assumption (iii) and because n is smaller than the boundary-layer thickness. Thus the pressure forces in the boundary layers are negligible, except where θ approaches $\frac{1}{2}\pi$. Equation (16) now gives $h = h(0) - v_c\{1 - \exp(-mn)\}$, and the condition (13) requires that $h(0) = -cmv_c = -v_c cM\cos\theta$. It follows that the total currents towards X per unit length of pipe are $(\sigma\eta)^{1/2}v_0(h_c - h_0)$, which is equal to $-(\sigma\eta)^{1/2}v_0 v_c$, in the boundary layer, and $-(\sigma\eta)^{1/2}v_0 v_c cM\cos\theta$ in the wall. The current in the layer is proportional to the core velocity, because the wall shear stress, proportional to (core velocity)/(layer thickness) and hence to (core velocity) × (normal field intensity), is balanced by the magnetic force on the layer, proportional to (current in layer) × (normal field intensity).

The core region

From assumption (iv) we have $\partial h_c/\partial X + P/M \doteqdot 0$, and hence $h_c = -PX/M$, since h_c is odd in X. This indicates that the current density in the core is uniform and parallel to the y-axis, and equal to $Pv_0(\sigma\eta)^{1/2}/Ma$. The electromagnetic force just balances the pressure gradient. Also, Δh_c vanishes, and (8) shows that, in the core, $v_z = v_c(Y)$, a function of Y only. The current in the core must all return in the two boundary layers and walls, as shown in figure 3. Across any section AB, remote from X or Y, the total core current per unit length of pipe is

$2X_0\,Pv_0(\sigma\eta)^{1/2}/M$, in which $X_0 = (1-Y^2)^{1/2}$, if we neglect the boundary-layer thickness in comparison with the length $2X_0$ of AB. Continuity of current flow, or of h, demands that $PX_0/M = v_c(1+cM\cos\theta)$, and hence that

$$v_c = \frac{PX_0}{M(1+cMX_0)}, \tag{17}$$

the required function of Y. Equation (17) ceases to be valid as Y approaches ± 1.

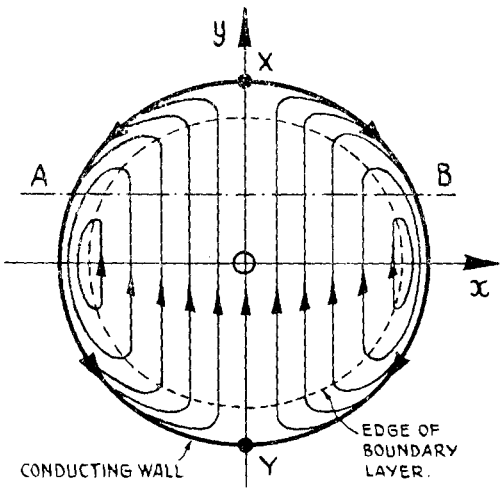

Figure 3. Current flow in walls, boundary layers and core.

The core velocity is not determined by local dynamical conditions, but indirectly by means of the current distribution. We may note in passing that when the walls are conducting, there is a downstream electromagnetic force on them with a corresponding net upstream force on the fluid. The pressure gradient has to counteract this as well as the viscous shear forces at the wall. When the walls do not conduct, there is no net electromagnetic force on the fluid. In neither case does the motion produce a force on the magnet supplying the transverse field, if edge effects are excluded.

It is now appropriate to examine some of the earlier assumptions. Equation (17) shows that Δv_c is of the order of P/M, and is negligible in (9), except when Y approaches ± 1. The boundary-layer thickness is small except where θ approaches $\frac{1}{2}\pi$. Obviously, the approximate treatment of the core and boundary layers fails near X and Y, but we assume that the solution is approximately valid elsewhere when M is large and the obscure regions are small.

Equation (17) is compatible with assumption (iii) provided cM is of the order of unity or less, and c is of the order of $1/M$ or less. For sodium flowing in a stainless steel pipe with reasonably thin walls, this condition is satisfied. The quantity cM is independent of the inside diameter of the pipe, and measures the relative conductivities of wall and boundary layer.

When cM is larger, the pressure gradient becomes important in the boundary layers, and the wall and core currents increase until the normal currents in the boundary layers become comparable with the tangential currents. Taking h as a function of n alone implies neglecting the normal currents.

Since the boundary layers are small, we may integrate (17) over the cross-section and relate P to the mean velocity v_0. This gives the relation

$$\frac{\partial p}{\partial z} = -\frac{3\pi\mu H_0 v_0(\sigma\eta)^{1/2}}{8a}(1+0{\cdot}883cM-0{\cdot}019(cM)^2+\ldots), \qquad (18)$$

which is nearly linear in cM.

The potential distribution may be found to the same accuracy from (11), in which $\mu H_0 v_z/(j_y/\sigma)$ is of the order of M. We therefore neglect j_y/σ and integrate along XY, assuming that no significant contribution to V_{XY} comes from the small obscure regions where v_z and j_y must be small. The variation of S with cM is shown in figure 4. When the walls are non-conducting, c vanishes and $S = 3\pi^2/32 = 0{\cdot}926$. Increasing the wall conductivity increases S, owing to the change in the velocity profile. Any decreasing tendency due to the short-circuit paths provided by the walls was neglected when j_y/σ was omitted from (11).

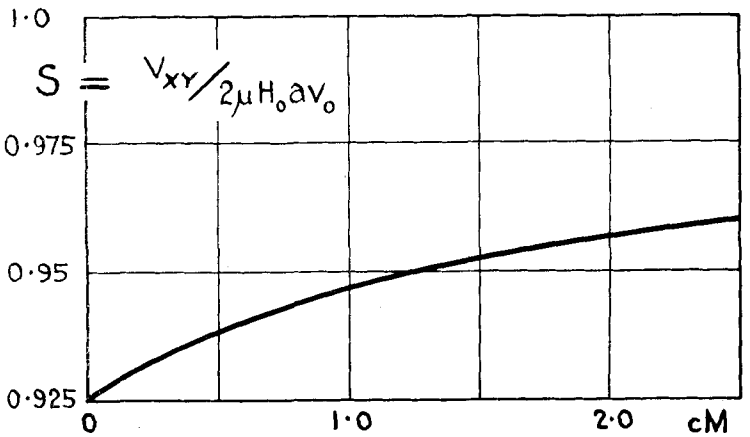

Figure 4. The effect of wall conductivity on sensitivity.

For low values of M, (8) and (9) may easily be solved in polar coordinates to yield solutions in series of ascending powers of M. In the steady state, the sensitivity is given by a series which begins with the terms

$$S = \frac{1}{1+c} - \frac{M^2}{576}\left(\frac{1}{1+3c}\right)+\ldots. \qquad (19)$$

4. The entry problem

The solution of (8) (less the β-term) and (9) is now considered for the case of a circular pipe with non-conducting walls, where the initial velocity is uniform and equal to v_0. It is not possible to impose an initial condition on h, since it is determined by (8). The spatial boundary conditions are that v and h shall vanish at the walls.

In order that the linear time-dependent case may be analogous to the original problem of entry into a region of transverse field, we must also impose the condition that v_0 and the integral of v over the pipe cross-section are constant.

It has been shown (Shercliff 1956) that when M is large and the fluid is flowing between parallel planes perpendicular to the field, a uniform entry-profile adjusts to its steady state in a dimensionless time T of the order of $1/M^2$. The dimensional time is of the order of $\rho/\mu^2 H_0^2 \sigma$, and the distance between the planes is irrelevant since the boundary-layer thicknesses are small in comparison. The settling process in this case simply involves the growth of boundary layers, the core velocity being virtually unaffected.

We should expect settling times for a circular pipe to be of the same order as for a square one, although somewhat less since the regions where the boundary layers are thick are smaller. For square pipes the dimensionless settling time is of the order of $1/M$ (Shercliff 1956).

The change from a uniform initial velocity in a circular pipe to the final steady profile, as already discussed, would be expected to fall into two stages as follows.

(*a*) During the first stage, lasting for a dimensionless time of the order of $1/M^2$, thin boundary layers are created as in the parallel-plane case, the core velocity being barely affected. Initially, no currents flow until viscous forces alone have produced a very small boundary layer. Subsequently, electromagnetic forces restrict the development of the layer to a thickness proportional to the reciprocal of the normal field intensity.

(*b*) In the second stage, occupying a much longer time of the order of $1/M$, the core profile is changed by electromagnetic forces to its final form, the boundary layer thickness being unchanged.

The motion in the regions near X and Y where the simple boundary layer theory fails is again left obscure on the assumption that the results are not seriously affected.

For both stages we shall make the following assumptions suggested by the steady state solution.

(i) M is large in comparison with unity.

(ii) The boundary layer thickness is always much smaller than a, so that all variables may be treated locally as functions only of T and n.

(iii) h and P/M are, at most, of the order of unity throughout. P may be related to the shear stresses at the walls by applying Green's theorem to the integral of (9) over the cross-section or the part in the first quadrant. This gives

$$\int_0^{\frac{1}{2}\pi} \frac{\partial v}{\partial n}\, d\theta = \frac{P\pi}{4}\,. \tag{20}$$

(iv) In the core, Δv_c is negligible in (9), and Δh_c is of the order of unity. The solution proves to be compatible with these assumptions except near X and Y. From (8) (less the β-term), it follows that $\partial v_c/\partial X$ is negligible and v_c is a function of Y and T only. We may note that this is true initially

and finally. Equation (9) degenerates to

$$M\,\partial h_c/\partial X + P = \dot{v}_c, \tag{21}$$

and we see that $\partial h_c/\partial X$ is also independent of X. Since h is odd in X, $\partial h_c/\partial X = h_c/X = h_0/X_0$, the value h_0 referring to the edge of the thin boundary layer. Equation (21) becomes

$$Mh_0/X_0 + P = \dot{v}_c. \tag{22}$$

On the basis of assumption (iii), this equation implies that $\dot{v}_c$ is of the order of M at most.

The first stage

This is expected to last a time of the order of $1/M^2$, and so the change in v_c will be of the order of $1/M$ and thus negligible. We shall therefore take v_c as unity during this stage.

Assumption (ii) applied to (8) and (9) for a point in the boundary layer on a radius vector inclined at an angle θ to the x-axis yields the equations

$$h'' - mv' = v'' - mh' - \dot{v} + P = 0. \tag{23}$$

Both h and v vanish when $n = 0$, and, when n is large, must approach the local core values h_0 and 1 respectively. From (23), $h' - mv = f(T)$, and hence $v'' - m^2v - v = mf(T) - P$ (independent of n) $= -m^2$, since when n is large, $v = 1$ and v'' and $\dot{v}$ vanish. In addition, $v = 1$ when $T = 0$. The solution is

$$v = 1 - \exp(-mn) + \frac{\exp(-m^2T)}{2(\pi m^2T)^{1/2}} \times \\ \times \int_0^\infty \exp(-u)\left[\exp\left(-\frac{(mn-u)^2}{4m^2T}\right) - \exp\left(-\frac{(mn+u)^2}{4m^2T}\right)\right] du,$$

in which the integral is obviously less than unity.

The form of the solution when T is a low multiple of $1/m^2$ is given closely by the first two terms. The boundary layer then resembles the steady-state one in extent, but the velocity rises to v_0 across every section of the layer. The first stage can be considered complete in a time of the order of $1/M^2$, even though $1/m^2$ is much larger in the obscure regions near X and Y.

Since P, which is of the order of M, is negligible in comparison with m^2 except near X and Y, then $f(T) \doteqdot -m$, and so $h' \doteqdot m(v-1)$. This equation and the condition $h = 0$ at the wall determine the behaviour of h, h_0 and hence h_c during the first stage. It can be shown that h_0 decreases steadily from zero, reaching -1 at the end of the first stage.

Figure 5 shows the current distribution at the end of the first stage. The boundary-layer current per unit length of the pipe is $(\sigma\eta)^{1/2}v_0$ at all sections of the boundary layer. There is singular behaviour near X and Y, where the currents issue into the core.

During the first stage, $\partial v/\partial n$ is of the order of m or M, except initially, when it is of the order of $T^{-1/2}$ and tends to infinity. Equation (20) shows

that P is, as assumed, of the order of M except when T is very small and M is an irrelevant variable.

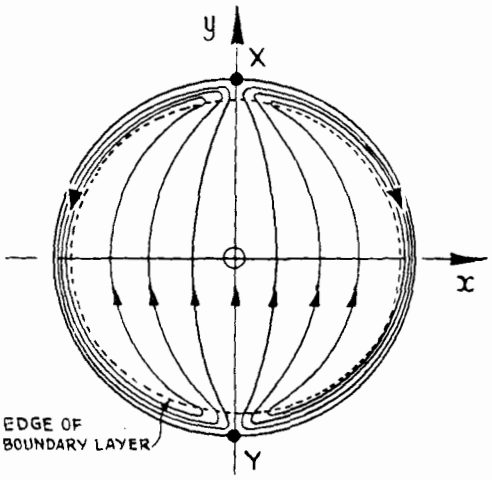

Figure 5. Current flow at the end of the first stage of the entry process.

The second stage

We shall see that v in the boundary layers is now of the same order as v_c. Hence $\dot{v}$ is, at most, of the order of M, and, like P, is negligible in (23). The boundary-layer analysis then gives $v = -h = v_c\{1-\exp(-mn)\}$, in which v_c varies with time, the extent of the boundary layers remaining constant. In particular $h_0 = -v_c$ and $\partial v/\partial n = mv_c$ at the wall. From (20) it follows that

$$P = \frac{4}{\pi}\int_0^{\frac{1}{2}\pi} M\cos\theta\, v_c\, d\theta = \frac{4M}{\pi}\int_0^1 v_c\, dY. \tag{24}$$

Again P is seen to be of the order of M. From (22) we may now deduce the linear equation

$$\frac{\dot{v}_c}{M} + \frac{v_c}{X_0} = \frac{4}{\pi}\int_0^1 v_c\, dY, \tag{25}$$

which governs the second stage of the motion. It is obvious that its duration will be of the order of $1/M$. The initial condition is $v_c = 1$, and no spatial boundary condition is necessary.

In calculating S we use (11) applied in the core, the term j_y/σ again being neglected. If no significant contribution to V_{XY} comes from the small obscure regions, it follows that

$$S = \int_0^1 v_c\, dY; \tag{26}$$

and we observe that P and S are simply proportional during the second stage. Equation (25) may be rewritten

$$\frac{\dot{v}_c}{M} + \frac{v_c}{X_0} = \frac{4}{\pi}S(MT), \tag{27}$$

which has the integrating factor $\exp(MT/X_0)$ and the solution

$$v_c = \exp(-MT/X_0)\left\{1+\frac{4}{\pi}\int_0^{MT} S(u)\exp(u/X_0)\,du\right\}$$

$$= \exp(-MT/X_0)+\frac{4}{\pi}\int_0^{MT} S(u)\exp\{(u-MT)/X_0\}\,du.$$

Application of the condition (26) yields the integral equation

$$S(MT) = H(MT)+\frac{4}{\pi}\int_0^{MT} S(u)H(MT-u)\,du, \tag{28}$$

where

$$H(p) = \int_0^1 \exp(-p/X_0)\,dY.$$

A numerical solution of (28) has been calculated, taking steps of 0·1 in MT and u. Initially S is unity, the velocity profile being almost wholly radially-symmetric (Kolin 1945); and finally the steady value $3\pi^2/32$ is reached. The continuous curve in figure 6 shows the variation of S or $-\{\pi a/4\mu H_0 v_0(\sigma\eta)^{1/2}\}\partial p/\partial z$ as a function of MT, or of Mz/Ra if we return to the non-linear entry problem by means of the Rayleigh approximation, setting $z = v_0 t$ and taking R to be the Reynolds number $\rho v_0 a/\eta$ based on pipe radius.

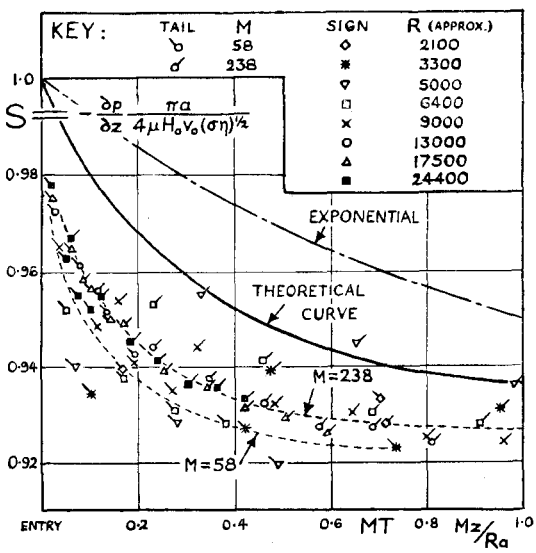

Figure 6. The entry process. S or dimensionless pressure gradient as a function of MT or Mz/Ra. The experimental points are from measurements of S at different values of M, R and z.

When T is small, the exact variation of S is not physically significant, because it is chiefly affected by the behaviour of v_c in the obscure regions near X and Y, and also because the first stage of the motion is still occurring. Moreover, the transverse field is not entered instantaneously in practice.

From figure 6 it will be observed that S is within 1% of its final steady value when $z \doteqdot Ra/M$. This makes an interesting comparison with the result for a rectangular pipe (Shercliff 1956) that departures from the ultimate steady velocity profile decrease by a factor $1/e$ in an entry length of the order of Ra/M. The departure of S from its ultimate value would be expected to decay similarly; and for comparison a chain-dotted exponential, decreasing by $1/e$ in a length Ra/M but having the terminal values appropriate to the circular case, has been added to figure 6. This emphasizes the fact that when M is large, entry lengths in rectangular pipes are considerably longer than in circular pipes.

The analysis has not been extended to cases where the entry velocity is not uniform. There is no reason for expecting the entry length to be very different. The analysis could easily be adapted for any initial variation of velocity in the y-direction. If the core velocity varies in the x-direction, such variations would probably be eliminated in the first stage by eddy currents in the xy-plane. This is suggested by the fact that for flow between parallel planes (Shercliff 1956), the entry length is of the order of Ra/M^2 when the core velocity varies in the x-direction.

Solutions in the form of series in ascending powers of M, valid when M is small, could be found, but the interest in such cases is slight.

Pressure loss at entry

In addition to the pressure loss due to the steady pressure gradient, there is a pressure loss δp associated with the profile adjustment from a uniform inlet velocity. No allowance will be made for the further large pressure loss due to eddy currents at the edge of the transverse field, as discussed by Hartmann (1937).

The drop δp may be found by integrating the excess of $\partial p/\partial z$ above its steady state value from zero to large values of z. No significant contribution comes from the very brief first stage of the motion, despite the singularity of P when $T = 0$. We can therefore use the second-stage result

$$P = 4MS/\pi. \tag{29}$$

From (27) we obtain

$$\frac{\partial(X_0 v_c)}{\partial(MT)} + v_c = \frac{4}{\pi} X_0 S,$$

which, when integrated from $Y = 0$ to $Y = 1$, shows that

$$\frac{\partial}{\partial T} \int_0^1 X_0 v_c \, dY = 0$$

because of (26). Hence

$$\int_0^1 X_0 v_c \, dY = \text{const.} = \tfrac{1}{4}\pi$$

initially, which expresses the equation of continuity since the boundary

layers are very thin. Also from (27), we get

$$\frac{\partial(X_0^2 v_c)}{\partial(MT)} + X_0 v_c = \frac{4}{\pi} X_0^2 S.$$

Integration of this equation from $Y = 0$ to $Y = 1$ gives

$$\frac{\partial}{\partial(MT)} \int_0^1 X_0^2 v_c \, dY = \frac{8S}{3\pi} - \frac{\pi}{4},$$

and hence

$$\frac{9\pi^2}{128} - \frac{2}{3} = \frac{8}{3\pi} \int_0^\infty \left(S - \frac{3\pi^2}{32}\right) d(MT),$$

since $v_c = 3\pi X_0/8$ finally, and the required integral has been determined. It follows that

$$\delta p / \tfrac{1}{2}\rho v_0^2 = \frac{27\pi^2}{128} - 2 = 0{\cdot}082,$$

which contrasts with the larger value 0·667 calculated by the Rayleigh approximation (Shercliff 1956) for flow into a circular pipe when magnetic effects are negligible. When M is large we see that δp is independent of M. A similar result would be expected for flow into rectangular pipes, in contrast with the result (Shercliff 1956) that $\delta p / \tfrac{1}{2}\rho v_0^2 = 1/M$ for flow between parallel planes when M is large. In this case there is no second stage of the motion, and δp is correspondingly smaller.

5. Experimental work

Experiments have been performed with the main object of verifying the theoretical values of S and $\partial p/\partial z$ in the steady flow of mercury in a non-conducting circular pipe under a transverse magnetic field at large values of M. The available values of M were limited by the saturation of the electromagnet and by the use of a tube small enough to produce measurable pressure gradients. Previous experiments (Hartmann and Lazarus 1937) reached a value of M of 18 only, and did not consider entry effects.

The apparatus also yielded approximate results for the variation of S and $\partial p/\partial z$ during the entry process, since only at the lower flow rates and greatest field intensities could steady conditions be reached within the extent of field available. At the lower flow rates and field intensities, the measured potential and pressure differences were liable to stray thermal and other effects, but nevertheless significant evidence in support of the theoretical work was obtained.

Experimental details

Figure 7 illustrates the mercury flow circuit schematically. The test-section indicated was either of two alternative Perspex pipes, installed in the gap of an electromagnet. One of 0·5 in. internal diameter with seven pairs of flowmeter-type electrodes at 1·5 in. pitch was used for measurements of S, and one of 0·25 in. diameter with four flush tappings at 3 in.

pitch for measurements of $\partial p/\partial z$. The electrodes were in fact small flush tappings also, this type having proved very successful. Tappings of $\frac{1}{32}$ in. diameter were the smallest that could be satisfactorily cleared of air. In each case the first tapping was 1·5 in. downstream of the edge of the magnet pole-faces.

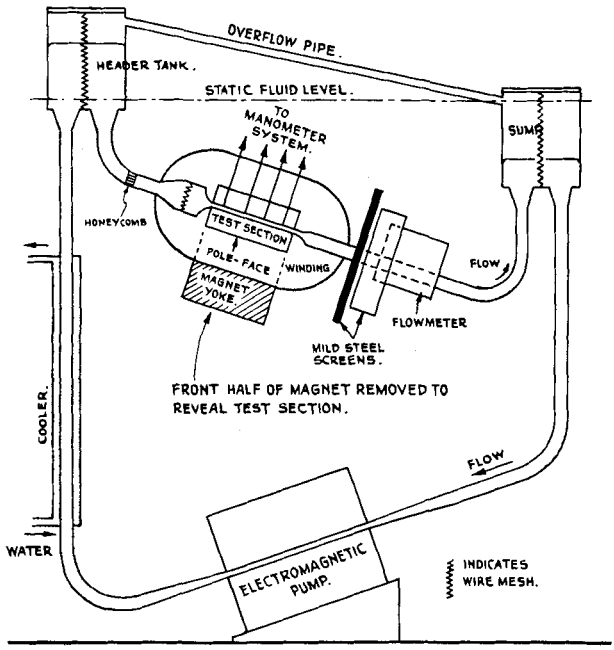

Figure 7. The fluid circuit (not to scale).

Steady flow occurred through the test-section under a gravity head of mercury maintained by an electromagnetic flat linear induction pump in the lower limb of the circuit. The cooler removed heat supplied by the pump. The mercury entered the test-sections through a streamlined contraction from a settling chamber with wire mesh grilles and preceded by a honeycomb to eliminate swirl. The velocity would presumably be nearly uniform after the contraction. Horizontal piping was avoided to aid the removal of air.

The flow rate was measured by an electromagnetic flowmeter in the upper limit of the circuit. Disturbance of this meter by the electromagnet was eliminated by the mild-steel screens shown and, when necessary, by taking the means of readings with the electromagnet energized alternatively in either direction.

The flowmeter was calibrated before and after the experiments with the screens in position using the apparatus illustrated in figure 8. The mercury flowed through the meter and the control cock under a constant head of 5·5 ft. Runs began when plug G was opened with plug H shut.

The mercury rose in the weir tank until a clock was started when contact was made with the electrode *Z*. This was surrounded by a sheath into which the mercury entered through a constriction at the bottom. The plug *H* was then opened, admitting mercury to the weigh tank until *H* was shut shortly before the header tank emptied. The clock stopped when contact was made at *Z* for the second time, there being the same amount of mercury in the weir tank at both timing instants. Thus the timed interval corresponded to the amount admitted to the weigh tank. After weighing, the mercury was blown back to the header tank through another pipe. Mercury has the advantage that electrical level indicators are easily arranged.

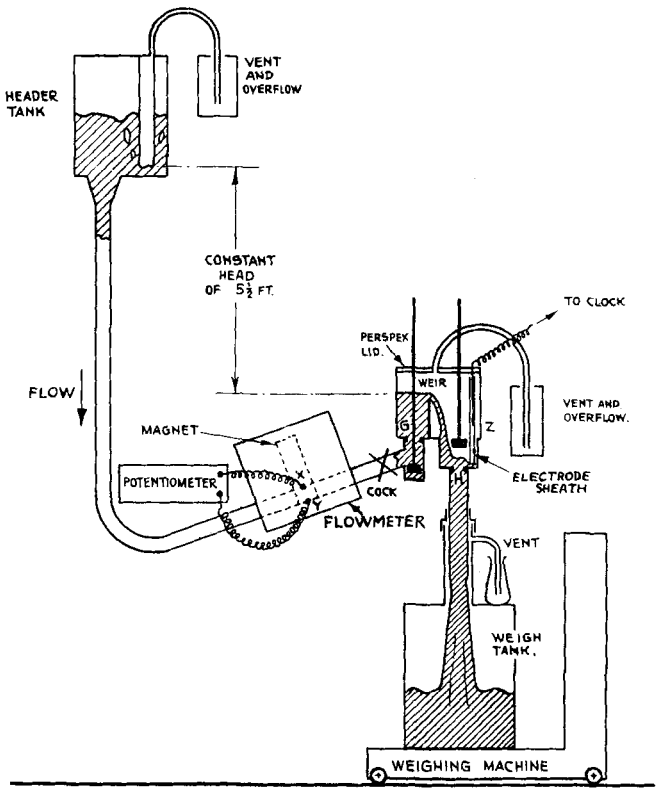

Figure 8. The flowmeter calibration rig (not to scale).

The apparatus worked well, even for runs as short as 18 sec. The flowmeter was found to give a relation between flow rate and output voltage which was linear over a wide range and reproducible within $\pm 0{\cdot}5\%$ of the mean in all positions relative to the upstream bend. This reliable calibration is to be attributed chiefly to the narrow fluid passage of the flowmeter, 1·10 in. deep and 0·04 in. in the field direction.

The electromagnet had pole faces 5 in. by 12 in. and a 1·25 in. gap. The water-cooled, low-voltage winding enabled fields of 14 800 oersted

to be attained. There was a sensibly single-valued relation between field intensity at the pole-face centre and exciting current for both directions of magnetization. Accordingly, the exciting current, measured in a temperature-insensitive shunt, was used to indicate field intensity after an initial calibration with a Cambridge fluxmeter and search coil had been performed. The experimental values of H_0 are considered accurate to 0·5%, except perhaps at low field intensities.

The field intensity fell off near the edges of the poles, the fall reaching 2% at the end electrode positions when the field was at its greatest value. A simple proportional correction was applied to voltages measured at the end electrodes, but not to the pressure differences. The effect of secondary currents at the field edges is difficult to allow for, but is small.

The test-section diameters were measured to 0·5% either by travelling microscope or weighing with a known length full of mercury. Mercury properties were taken from the *Liquid Metals Handbook* (Lyon 1952) and corrected for temperature changes.

All signals from the various electrodes were measured to 1 or 2 microvolts with a potentiometer, the readings at the higher flow rates or lower fields being more uncertain owing to increased unsteadiness of the flow. Care was necessary to ensure that the leads to the test-section electrodes did not link any of the main field as otherwise its small variations would produce large spurious signals. This is a point in favour of permanent magnets for flowmeters. Slight thermo-electric effects were observed when the magnet was running warm. All runs involving small signals were therefore made before the magnet had become warm.

Pressure gradients were measured with the sensitive manometer illustrated in figure 9. This instrument could record pressure differences to 0·001 in. of methylated spirits, a better fluid than water which is liable to wet non-uniformly. Owing to the presence of a warm magnet, however, it was impossible to eliminate stray errors of the order of 0·002 in., despite thorough lagging.

The four pipes from the flush tappings in the test-section led to the eight pinchcocks, which enabled the pressure difference between any two tappings to be measured, and also the 'zero' reading of the manometer to be established at any time. The manometer itself consisted of an inverted U-tube containing air above spirits. The spirits/mercury menisci were kept at fixed levels in reservoirs of large area by taking all readings with the air/spirits menisci brought to fixed positions in the two sloping parts of the U-tube. This also eliminated surface tension errors. It was achieved by adjusting the volume of air above the spirits and by altering the height of the right-hand sloping tube. Changes in the volume of the flexible tube below this had negligible effect, and thermal and other effects were reduced by the near-symmetry of the manometer system. A micrometer screw recorded the change in height of the sloping tube. The 'zero' reading was taken repeatedly as it was found to drift during long runs. The manometer took about 15 min to reach a steady state.

As the micrometer travel was limited, to measure the larger pressure differences the manometer was converted to a spirits/mercury one by allowing the spirits to rise, expelling the air, until the mercury menisci were in the sloping tubes. Readings taken by both methods were consistent. The smallest heads that were measured were about 0·05 in., read to the nearest 0·001 in. Care was taken to keep the mercury in the circuit at ambient temperature to minimize hydrostatic errors in the inclined test section.

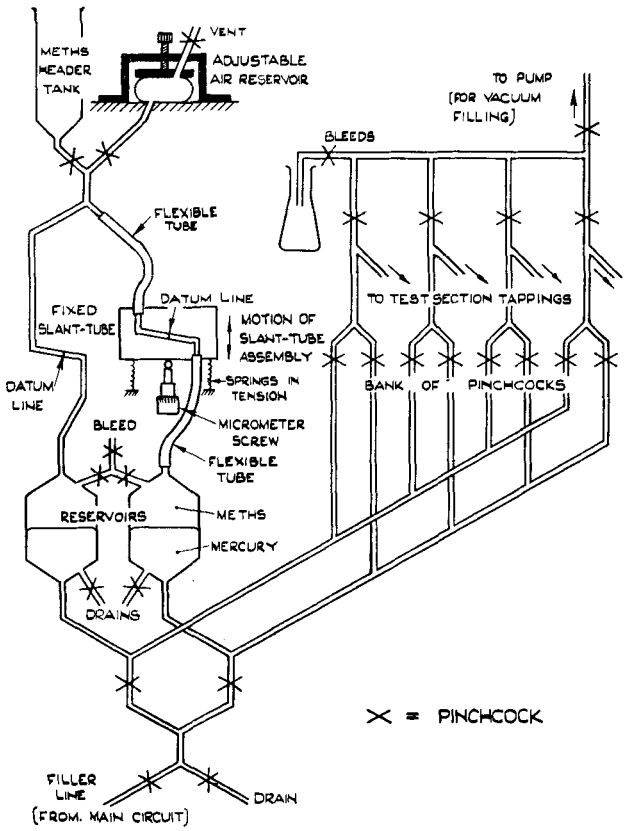

Figure 9. The manometer system, showing the air/methylated spirits arrangement (not to scale).

Observations were taken at four electromagnet field intensities and a range of flow rates, each 50% higher than the previous one. The upper limit was set by the available head, and the lower by the smallness of the signals to be measured by the potentiometer in the presence of stray potentials. The lowest signals were measurable only to 2% accuracy.

Experimental results: pressure gradients in the 0·25 *in. tube*

Figure 10 shows the readings reduced to dimensionless form, the three measured mean gradients between tappings being expressed as a multiple

of the theoretical gradient $3\pi\mu H_0 v_0(\sigma\eta)^{1/2}/8a$, valid for steady conditions when M is very large. Flow rate is represented by R, the Reynolds number based on radius. There are three zones in which the constant-M curves are horizontal, rising slowly and rising precipitately.

Where the experimental points are all marked as crosses, the three pressure differences showed a scatter but no clear falling tendency along the pipe. The central pressure difference tended to be slightly high. Horizontal lines fit the points reasonably well, and we deduce that this zone corresponds to steady flow that is laminar, because the gradient is independent of R and density.

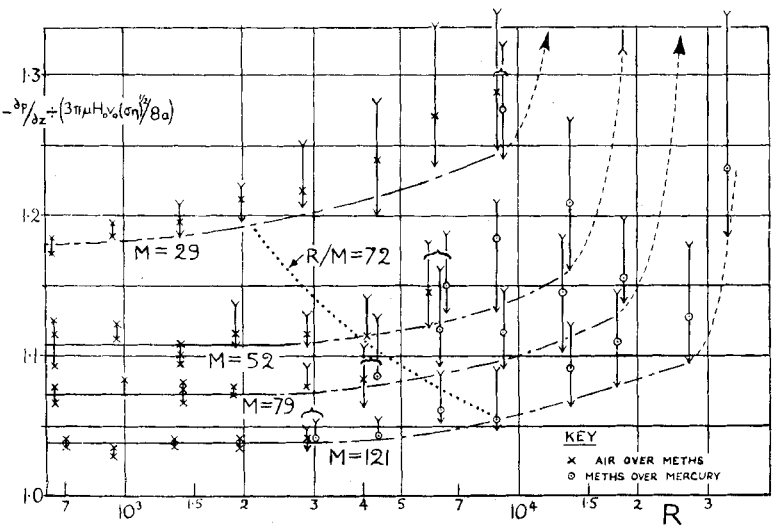

Figure 10. Experimental values of pressure gradient plotted non-dimensionally against flow rate at four field intensities.

At higher flow rates the pressure gradient was observed to fall along the pipe as steady conditions were approached, and here the three successive points are marked as arrow tail, cross (air/spirits) or circle (spirits/mercury) and arrow head. The points suggest that the flow was approaching a steady state with the same value of $(\partial p/\partial z)/(3\pi\mu H_0 v_0(\sigma\eta)^{1/2}/8a)$ as for the lower flow rates. Chain-dotted curves connect the arrow heads approximately. When M was 29, steady conditions were barely obtained even at the lowest flow rate. The pairs of arrows linked by brackets represent the fastest air/spirits readings and the slowest spirits/mercury readings, consistent within experimental error. During the runs where a steady state was still being approached, the readings both of pressure gradient and voltage were particularly prone to wander, even though the total flow rate was steady.

Finally the pressure gradients are seen to rise rapidly at a value of R that increases with M. Most of the experimental points are off the figure.

With $M = 29$ or 52 the gradients increased along the tube. There seems to be no doubt that a transition to turbulence was being observed. The rig did not permit an adequate study of the turbulent regime, and this was not attempted. It appears that provided $R < 250M$ approximately, laminar flow occurred under the conditions of the experiment, and that, in particular, there was laminar flow in all the runs with the 0·5 in. tube, described in the next section, except perhaps the fastest runs at the lowest field strength.

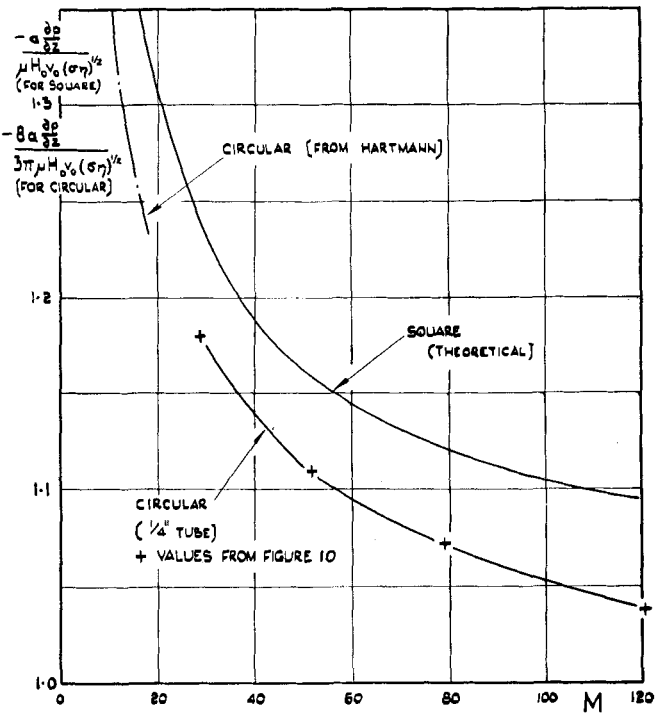

Figure 11. Ultimate pressure gradient plotted non-dimensionally against M for circular and square tubes.

The four steady values of $(\partial p/\partial z)/(3\pi\mu H_0 v_0(\sigma\eta)^{1/2}/8a)$ taken from figure 10 are plotted against M in figure 11. It appears likely that the curve does approach the value unity asymptotically as M increases. Experiments at higher values of M would almost inevitably involve the use of liquid sodium. Figure 11 also includes an approximate chain-dotted curve taken from the experiments of Hartmann & Lazarus (1937) for values of M up to 18. This is clearly compatible with the new results.

Experimental results: potential differences across the 0·5 *in. tube*

Values of S calculated from readings at the seven electrode pairs are plotted in figures 12(*a*) and 12(*b*) for values of M of 239 and 58. Similar intermediate results were obtained with M equal to 156 and 102. Curves

have been added to illustrate the trend of the results as R varies. The caption 'entry' refers to the leading edge of the pole faces.

Attention is directed first to figure 12 (*a*), since the readings are most reliable at the highest field strength. It is apparent that at the lower flow rates steady conditions were reached within the test-section, and that S then assumed the approximate value 0·92, confirming theoretical expectations reasonably well. At higher flow rates, decreasing values of S closer to unity occurred, as expected, because the velocity profile was not fully distorted from its presumed initial axial symmetry in the length available.

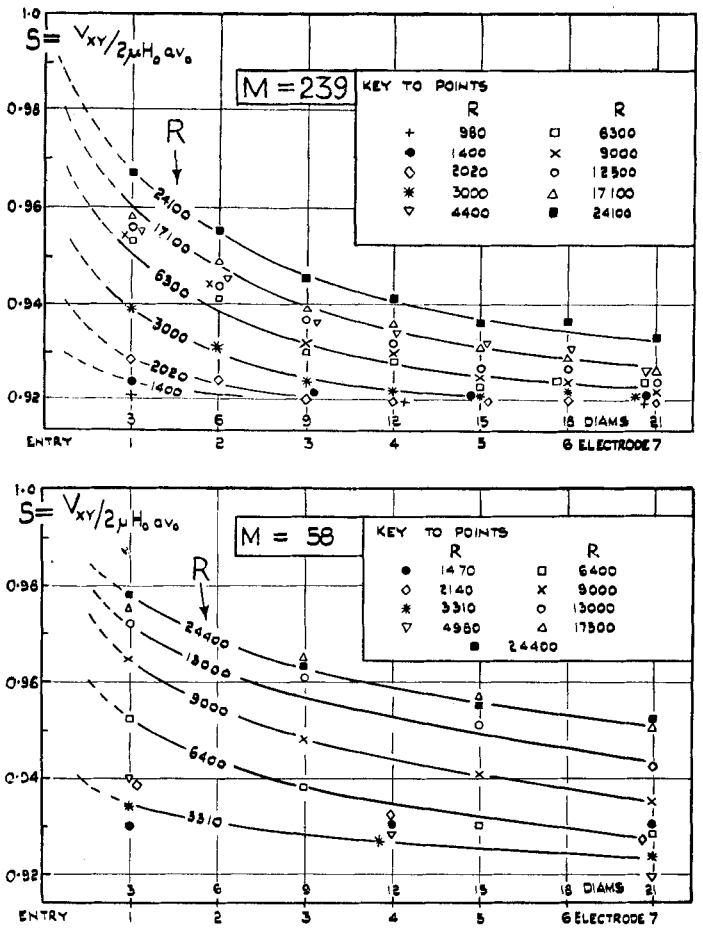

Figure 12. The fall in sensitivity along the 0·5 in. pipe.
(*a*) $M = 239$, (*b*) $M = 58$.

The accuracy fell as the field was reduced owing to the smallness of the quantities measured. Nevertheless figure 12 (*b*) is consistent with theoretical expectations. Another difficulty was the unsteadiness of the flow in runs where the settling process was protracted. It was impossible to achieve precise reproducible trends in these cases.

The entry process

The scatter of the results makes a close experimental check of the entry theory difficult. It is also complicated by the uncertainty of the entry conditions. As the streamlined contraction terminated about 1·25 in. before the edge of the pole-faces, there would presumably be some distortion of the velocity profile caused by the fringe flux before the main field was entered, and moreover the secondary currents at the field edges tend to distort the velocity profile. Nevertheless, in order to check the entry theory (itself approximate) we shall assume conventionally that the velocity was uniform at the section opposite the edge of the pole faces, and measure z from this section.

Experimental points for values of M of 239 and 58 have therefore been plotted in figure 6, z being measured from the edge of the pole faces. Dotted mean curves have been added. The theoretical entry length is seen to be correct in order of magnitude, if considerably overestimated. The experimental points also tend to confirm that the sensitivity S started to fall from unity while z was still negative.

A closer investigation of the entry process would require an elaborate technique to secure known, standard entry conditions. The dependence of S on the velocity profile provides a useful technique for studying such phenomena as the pipe-entry process, unless the velocity profile is radially symmetric.

Equation (28) indicates that $\partial p/\partial z$ and S should be mutually proportional at high values of M (except perhaps when the entry length is so long that the first stage with its higher value of $\partial p/\partial z$ becomes important). There is rough confirmation of this result in that $\partial p/\partial z$ and S both fall by amounts as large as 8% during the settling process. Figure 6 shows that S is usually within 1% of the steady state value when $Mz/Ra = 1$. A dotted curve for which $R/M = 72$, the value of z/a which corresponds to a point midway between the last two pressure tappings in the 0·25 in. tube, has therefore been added to figure 10. It is found to connect points where $\partial p/\partial z$ is roughly 1% above the steady state value. Thus both sets of readings give entry lengths of the same order of magnitude.

As M increases, the steady state value of S approaches its asymptotic value more rapidly than $(\partial p/\partial z)/(3\pi\mu H_0 v_0(\sigma\eta)^{1/2}/8a)$ tends to unity, simply because S (unlike $\partial p/\partial z$) only varies through a small range over the whole range of M. It was clearly impossible to find the variation of S with M from the present experiments. Hartmann & Lazarus did not measure potentials.

For comparison, a theoretical curve (Shercliff 1953) showing the variation of the steady $(\partial p/\partial z)/(\mu H_0 v_0(\sigma\eta)^{1/2}/a)$ against M for a square pipe of side $2a$, with the field parallel to a side, has been added to figure 11. This curve approaches the value unity less rapidly than the experimental curve for the circular pipe, presumably because the regions where the boundary layers are thick are smaller in circular than in square pipes.

6. Practical implications

It has been shown that distortion of the velocity profile can cause the sensitivity of a flowmeter of circular section to fall from the Kolin value by about 8%, provided the fluid traverses the magnetic field for a distance at least equal to Ra/M before encountering the electrodes, the theoretical distance being somewhat larger than the observed ones. It is important to consider whether the fall will occur commonly in practice. Typical figures for a small flowmeter of 1 in. bore bearing liquid sodium at 300° C at 100 cm/sec in a field of 3000 oersted are $R = 3{\cdot}3 \times 10^4$, $M = 500$ and $R/M = 66$. Since the field would probably extend for 2 or 3 rather than 33 diameters upstream of the electrodes, we see that only at much lower flow rates would appreciable distortion of the velocity profile and fall in sensitivity occur. Variation of sensitivity due to upstream disturbances or edge effects is likely to be much more serious (Shercliff 1954, 1955).

Further experiments to test the variation of S with wall conductivity would be interesting, but also very difficult owing to the importance of contact resistance.

The experiments described above were carried out with the help of facilities provided at Cambridge University by the Atomic Energy Research Establishment, Harwell.

References

Bullard, E. C. 1955 *Proc. Roy. Soc.* A, **233,** 289.

Hartmann, J. 1937 *Math.-fys. Medd.* **15,** No. 6.

Hartmann, J. & Lazarus, F. 1937 *Math.-fys. Medd.* **15,** No. 7.

Kolin, A. 1945 *Rev. Sci. Instr.* **16,** 109.

Lock, R. C. 1955 *Proc. Roy. Soc.* A, **233,** 105.

Lyon, R. N. 1952 *Liquid Metals Handbook,* Navexos P-733, U.S. Office of Naval Research.

Murgatroyd, W. 1953 *Phil. Mag.* **44,** 1348.

Shercliff, J. A. 1953 *Proc. Camb. Phil. Soc.* **49,** 136.

Shercliff, J. A. 1954 *J. Appl. Phys.* **25,** 817.

Shercliff, J. A. 1955 *J. Sci. Instr.* **32,** 441.

Shercliff, J. A. 1956 *Proc. Camb. Phil. Soc.* **52,** 573.